First lasing in an infrared free electron laser at RRCAT, Indore

K. K. Pant[1,*], Vinit Kumar[1,2], Bhaskar Biswas[1], Arvind Kumar[1], Shankar Lal[1], Sona Chandran[1], Saket Kumar Gupta[1], Md. Khursheed[3], Pravin Nerpagar[1], A. K. Sarkar[1], Ravi Kumar Pandit[1], K. Ruwali[4], K. Sreeramulu[4], S. Das[4], R. S. Shinde[4], S. Chouksey[5], J. K. Parate[5], Viraj Bhanage[6], P. P. Deshpande[6], Shradha Tiwari[6], Mandar Joshi[7], Lalita Jain[6], Anand Valecha[8], Ayukt Pathak[6], M. A. Ali[6], H. R. Bundel[6], Purushottam Shrivastava[9], T. Reghu[9], Umesh Kale[9], Yashwant Wanmode[9], Praveen Mohania[9], Jaikishan Mulchandani[9], Akhil Patel[9], Mahesh Acharya[9], Ashish Mahawar[9], Mahendra Lad[10], M. K. Jain[10], Nitesh Tiwari[10], Pritam S. Bagduwal[10], V. G. Sathe[11], Sujata Joshi[11], Ram Shiroman[11], A. S. Yadav[11], Randhir Kumar[11], Alok Singh[12], Vineet K. Dwivedi[12], Mangesh Borage[2,12] and S. R. Tiwari[12]

[1]Materials and Advanced Accelerator Sciences Division,
[2]Homi Bhabha National Institute,
[3]Advanced Lasers and Optics Division,
[4]Accelerator Magnet Technology Division,
[5]Design and Manufacturing Technology Division,
[6]Laser Controls and Instrumentation Division, Raja Ramanna Centre for Advanced Technology, Indore 452 013, India
[7]Laser and Plasma Technology Division,
Bhabha Atomic Research Centre, Mumbai 400 085, India
[8]Accelerator Control Systems Division,
[9]Pulsed High Power Microwave Division,
[10]Radio Frequency Systems Division,
[11]Ultra-High Vacuum Technology Division, and
[12]Power Converters Division, Raja Ramanna Centre for Advanced Technology, Indore 452 013, India

An Infrared Free Electron Laser (IR-FEL) designed to operate in the 12.5–50 μm wavelength band is presently in an advanced stage of commissioning at the Raja Ramanna Centre for Advanced Technology (RRCAT), Indore. Here we report results from first experiments on the IR-FEL after installation of its optical cavity, which has resulted in a power output that is ~10^5 times the expected spontaneous emission power for the beam parameters used in the experiment. The estimated out-coupled peak micro-pulse power during these experiments is ~2 kW. This is the first observed signature of lasing in the IR-FEL, and the first reported lasing in a FEL in India. This communication discusses the development of the IR-FEL, the recent experimental results, and the ongoing efforts to further increase the IR power to the design peak out-coupled power of 2 MW.

Keywords: Beam parameters, free electron laser, infrared power, undulator.

FREE electron lasers (FELs) are accepted worldwide as state-of-the-art tools for cutting-edge research in different areas of science and technology using short pulse and high power electromagnetic radiation. More than 50 FELs have been built worldwide spanning the complete electromagnetic spectrum[1], with the emphasis being on those operating in the X-ray region or in the long wavelength region covering the mm waves to mid-infrared region, where conventional lasers either do not exist with the desired operating parameters, or are not very competitive.

An Infrared Free Electron Laser (IR-FEL) designed to lase in the 12.5–50 μm wavelength band is presently in an advanced stage of commissioning at RRCAT, Indore. This FEL is designed to deliver a train of 10 ps pulses with ~2 MW peak power at a repetition rate of 29.75 MHz for a macro-pulse duration of a few microseconds, repeating at 1–10 Hz (ref. 2). This FEL is being built to serve as a user facility, where initial experiments have been planned on the study of materials in low temperature and high magnetic field environment. Almost all the subsystems of the IR-FEL have been developed in-house, with some help of the local industry. The indigenous plane wave transformer (PWT) linac structures employed in the injector system are high-gradient structures, and to the best of our knowledge, the IR-FEL at RRCAT is the only FEL worldwide built using PWT linac structures. A fast-pulsed thermionic electron gun, a 25 MW peak power klystron and its associated high-power microwave line components, and a 2.5 m long, pure permanent magnet undulator have been procured and installed in the IR-FEL set-up. Figure 1 shows the design layout of the IR-FEL set-up with the injector on the left followed by the electron beam transport line leading to the undulator and the optical cavity, and the beam dump at the extreme right. Here, 'sol' refers to the solenoid magnets in the low-energy electron beam transport line, and 'BM' and 'QP' refer to bending magnets and quadrupole magnets respectively.

As the IR-FEL has been designed to operate in an oscillator configuration, stability of the accelerated electron beam in terms of jitter in mean energy and time of arrival of each 10 ps micro-bunch at the undulator entry are crucial to ensure overlap of successive electron micro-bunches with the optical radiation pulse bouncing back-and-forth repeatedly inside the optical cavity. Table 1 summarizes the IR-FEL design parameters, and the required electron beam and undulator parameters dictated by the FEL design simulations. The stability of the electron bunches from the IR-FEL injector system depends upon the stability of the 90 keV electron beam from the

*For correspondence. (e-mail: kkpant@rrcat.gov.in)

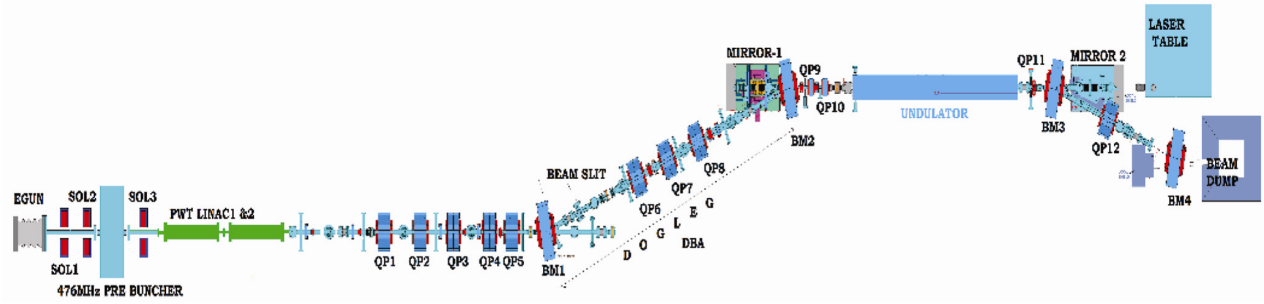

Figure 1. Design layout of the infrared free electron laser.

Table 1. Important design parameters of the infrared free electron laser (IR-FEL)

Design wavelength	12.5–50 μm
Design electron beam energy	15–25 MeV
Peak/average out-coupled power @ 10 Hz	2 MW/30 mW
Peak current	>30 A
Emittance (RMS, normalized)	30 mm mrad
Relative energy spread (RMS)	<0.5%
Mean energy jitter	<0.2%
Undulator period/length	5 cm/2.5 m
RMS undulator parameter K_{RMS}	1.2 at 27 mm gap

electron gun, and on the amplitude and phase stability of the high-power RF and microwave systems for the sub-harmonic pre-buncher and the PWT linac structures. The IR-FEL injector employs subsystems at three different frequencies: electron gun at 29.75 MHz, subharmonic pre-buncher at 476 MHz and PWT linac structures at 2856 MHz. Synchronous generation and amplification of signals at these frequencies with the required amplitude and phase stability is critical for lasing of the IR-FEL.

The injector system for the IR-FEL employs a thermionic electron gun that was custom-built by a vendor according to our design specifications, followed by a sub-harmonic pre-buncher structure and two cascaded PWT linac structures, all built in-house. The fast-pulsed thermionic electron gun delivers 90 keV bunches of 1 ns full-width-at-half-maxima (FWHM) pulse width and 1 nC charge, repeating at 29.75 MHz for a macro-pulse duration of 1–10 μs. The 29.75 MHz repetition rate of the gun is chosen to match the spacing between the electron micro-pulses with the round-trip time of optical pulses inside the 5.04 m long optical cavity of the IR-FEL for lasing to build-up. Each 1 ns long electron bunch from the electron gun is bunched to ~50–80 ps by a sub-harmonic pre-buncher structure before injection into two cascaded 12-cell PWT linac structures for further bunching and acceleration to the rated electron beam energy of 15–25 MeV (ref. 3). The sub-harmonic pre-buncher is a single-cell structure with a re-entrant geometry. It imparts a ~17 keV energy modulation to the 90 keV electron bunches from the electron gun, leading to their bunching-to ~50–80 ps at the entry port of the linac. Each PWT linac structure employed in the IR-FEL injector system has 12 cells with an RF length of 63 cm, and is capable of imparting an energy gain of 9–10 MeV consuming between 4 and 5 MW of peak RF power. The open geometry of a PWT linac structure makes it different from the conventional SLAC-type linac structures, and the high inter-cell coupling coefficient in this structure makes it more tolerant to machining imperfections. A low-energy electron beam transport line comprising three solenoid magnets is employed to transport the 90 keV electron beam from the gun to the entry port of the first PWT linac, with steering magnets for correction of trajectory.

The pre-buncher and PWT linac structures have been built to operate stably at the design accelerating electric field gradients without any significant frequency drift due to thermal effects. These PWT linac structures have been operated at a reasonably high accelerating gradient of ~19 MV/m to deliver an 18.2 MeV electron beam that is presently used in experiments to lase at ~34 μm wavelength. Employing two cascaded linac structures in the place of one long linac structure imposes an additional requirement of precise phase control and stabilization between the two structures for consistent operation of the injector system, which has successfully been demonstrated in the IR-FEL injector system.

An RF synchronized signal generation unit has been developed in-house to generate synchronized signals of 29.75 MHz for the electron gun, 476 MHz for the sub-harmonic pre-buncher and 2856 MHz for the PWT linac structures. The synchronized LLRF signals at 476 and 2856 MHz are then fed to two amplifier systems that amplify them to the power levels required for the sub-harmonic pre-buncher and linac structures respectively, viz. 10 kW peak power at 476 MHz and 15 MW peak power at 2856 MHz. This synchronized signal generation unit also generates a 10 MHz reference signal for the trigger delay generation unit to keep the trigger signals for different subsystems in sync with the reference RF signal.

The RF power amplifier at 476 MHz for the sub-harmonic pre-buncher has been designed using a planar triode tube, and is housed in a standard 19 inch rack with all associated power supplies, matching circuits and cavity assemblies. Matching of the output network has been

achieved using a rectangular waveguide output cavity, with a tuning range of ±50 MHz. The input matching and tuning network has been realized using a strip line-based network with the required frequency tuning range. The amplifier employs an 8.0 kV modulator DC power supply for the anode and a 90 V power supply with negative polarity for the grid. A Siemens-make PLC-based control, interlock and monitoring system is used for monitoring various parameters, and to facilitate proper startup and shutdown of the amplifier system. This system also detects malfunctions during operation and brings the system to a safe stage, thereby assuring reliable operation of the amplifier system. A detector board using RF detector (ZX-47), sample and hold (LF398) and mono stable IC (CD4538) has been developed to measure peak pulse RF power sampled from a directional coupler.

To achieve a stable RF gap voltage and phase in the pre-buncher cavity, a PXI-based pulsed digital LLRF control system has been developed, which provides high accuracy of the RF cavity field control with a higher dynamic range, in addition to the inherent feature of flexibility, adaptability and reduced long-time drift errors. The system has been developed in-house using XILINX-make FPGA-based digital electronics[4], and a graphical user interface (GUI) has been developed for operation of the RF system and for measurement of various operating parameters. Digital I/Q detection has been used for amplitude and phase detection, and the controller has been implemented in Virtex-5 FPGA.

Testing of the digital LLRF system and the pulsed RF amplifier was done by powering the pre-buncher cavity initially in an open-loop configuration for measurement and calibration of the RF cavity gap voltage, RF phase and RF power. Subsequently, the parameters of the digital feedback controller were optimized in close-loop operation to achieve the required electric field amplitude and phase stability. With the optimized operating parameters, the 476 MHz pulsed RF system was tested at full power of 10 kW with 50 μs RF pulse width at the required repetition rate of 10 Hz. The required stability of ± 0.1% in amplitude and ±0.1° in phase was achieved for the RF field in the pre-buncher cavity.

The S-band microwave system for the IR-FEL employs a 25 MW peak power klystron and a line-type pulse modulator with two tuneable pulse-forming networks (PFNs) in parallel, a 50 kV capacitor charging power supply and a thyratron switch. The high-voltage deck is an oil-filled tank with an indigenously developed high-voltage pulse transformer with a turn ratio of 1 : 14. The klystron and the focusing electromagnets are also part of the high-voltage deck. A WR-284 waveguide line pressurized at 2 kgf/cm^2 with sulphur hexafluoride (SF_6) gas is used to transfer power from the klystron to the two PWT linacs through a 3 dB power splitter. Figure 2 shows a typical modulator output voltage waveform with flatness of ±0.35%.

An S-band LLRF system has been designed and developed for phase and amplitude stabilization of the S-band microwave power, which controls the microwave input to the 200 W solid-state driver amplifier for the klystron. This system uses analogue phase shifters and voltage variable attenuators to control the phase and amplitude respectively. The system includes feed-back capability to correct the phase and amplitude drifts occurring due to thermal variations, as well as a fast feed-forward mechanism to vary the amplitude and phase of the output pulse to compensate for beam loading and to shape the klystron output pulse shape. A programmable function generator has been used to generate the feed-forward waveform, which is then fed to the phase shifter and attenuator for pulse shaping[5].

While lasing of the IR-FEL is critically dependent upon the quality of its RF system, it also depends upon the stability of the electron beam transport system that is used to transport and manipulate a round beam of 'root mean square' (RMS) size of 2.5 mm at the exit of the injector linac system to a flat beam with RMS size 0.5 mm vertical) × 1.5 mm (horizontal) at the undulator entry. This transport system also includes an energy-selecting slit after the first bending magnet to select electrons with an RMS energy spread <0.5% about the mean energy. For efficient energy exchange between the electrons and the electromagnetic radiation inside the undulator, it is essential that the trajectory of the electrons is coincident with the axes of the undulator and the optical cavity. The tolerance on this alignment as prescribed by FEL simulations is ± 200 μm over the 5.04 m length of the optical cavity, with an angular tolerance of ±50 μrad. The trajectory of the electron beam inside the optical cavity has been successfully controlled to fall within this tight tolerance band during experiments, which was facilitated by the good field quality generated by the magnets, stable magnet power supplies (±50 ppm)[6], and a stable supervisory control and data acquisition (SCADA) system for the IR-FEL, all built in-house.

The IR-FEL electron beam transport line has been designed with a dog leg-type bend to fit the machine inside the 5 m width of a 60 m long shielded area. This transport line from the linac exit to the beam dump was designed using the TRANSPORT code[7,8]. Provision has been made in the transport line for movable slits after the first dipole for energy selection. The small achieved value of the R_{56} parameter (R_{56} = –0.01006 cm/% at 17.6 MeV) helps in preserving the peak current from the linac, which is crucial for lasing in the IR-FEL. Lasing in an FEL has been reported in the literature to cause an increase in relative energy spread in the electron bunch. To estimate the growth in beam size in the undulator region on account of this energy spread due to lasing, TRANSPORT simulations have been performed by modelling the undulator as a series of dipole magnets followed by short drift spaces. Energy spread of 2%, 3%

and 4% is introduced stepwise in these simulations at distances corresponding to ~$L/9$, $L/4$ and $L/2$ respectively, of the undulator length L. The horizontal beam size inside the undulator is observed to increase in this case, and the effect is amplified up to the beam-dump. Figure 3 shows the horizontal and vertical beam sizes at different locations along the IR-FEL beam transport line. The vacuum beam-line components on the dump side have been built with a large horizontal dimension, and suitable focusing and bending magnets have been deployed to ensure minimum beam loss. Eighteen beam profile monitors have been installed in the IR-FEL set-up from the electron gun to beam-dump for viewing the electron beam profile, and for measurement of electron-beam properties at different locations. The IR-FEL electron-beam transport system comprises 12 quadrupoles, four dipoles of 22.5° bend and 16 steering magnets in the high-energy section, and 3 solenoids and four steering magnets in the low-energy section. Specially designed compact quadrupole and steering magnets have been employed in the optical cavity region, where space is a severe constraint. All the quadrupole and dipole magnets have been mapped and fiducialized before installation in the IR-FEL set-up[9].

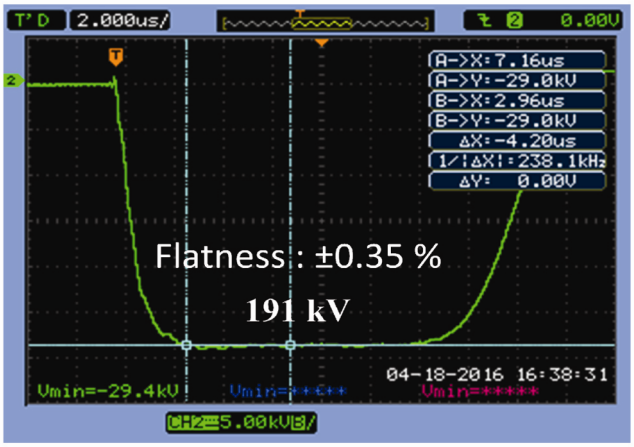

Figure 2. Typical modulator output pulse waveform.

Switch-mode, current-regulated power converters have been developed to energize the electromagnets of the electron beam transport line. These are rated for 13 A and 15 V (maximum) with output current stability of ±100 ppm, and are based on two-switch forward converter operating with variable frequency pulse width modulation (VFPWM) control in the range from 20 to 100 kHz. In all, 60 power converters, including spares, have been developed and presently, 45 power converters have been installed and commissioned. All associated low-power electronics, e.g. sensing, fault-handling, auxiliary power sources, handling remote interface has been standardized. Each power converter is standardized on a 6U card and five such power converters are housed in one 6U, 19 inch sub-rack. Three sub-racks are mounted inside a 36U cabinet. Some of the power converters are also equipped with polarity reversal switches[6]. This concept, design and architecture facilitated speedy development with industry support.

Commissioning of the IR-FEL beam transport line was started with a beam energy of 14 MeV. It has been successfully tuned to transport electron beam up to 19 MeV energy for the ongoing set of experiments with relative energy spread selection variable from ±0.5% to ±1%.

The IR-FEL employs a 2.5 m long, pure permanent magnet undulator procured from M/s Kyma srl, Italy. Table 2 provides details of the parameters of the undulator. The undulator magnetic field was qualified through in-house mapping using a Hall probe-based set-up and a stretched wire set-up before installation in the IR-FEL set-up. Figure 4 shows a plot of the undulator magnetic field mapped in-house before its installation in the IR-FEL set-up (red), and the undulator magnetic field mapped by the supplier, M/s Kyma srl (blue) before shipping it to RRCAT.

The complete IR-FEL set-up with a total length of ~17 m is maintained at a vacuum level $\leq 3 \times 10^{-9}$ mbar. Several electron beam diagnostic elements like beam viewers, integrating current transformers (ICTs) and beam position monitors (BPMs) have been incorporated

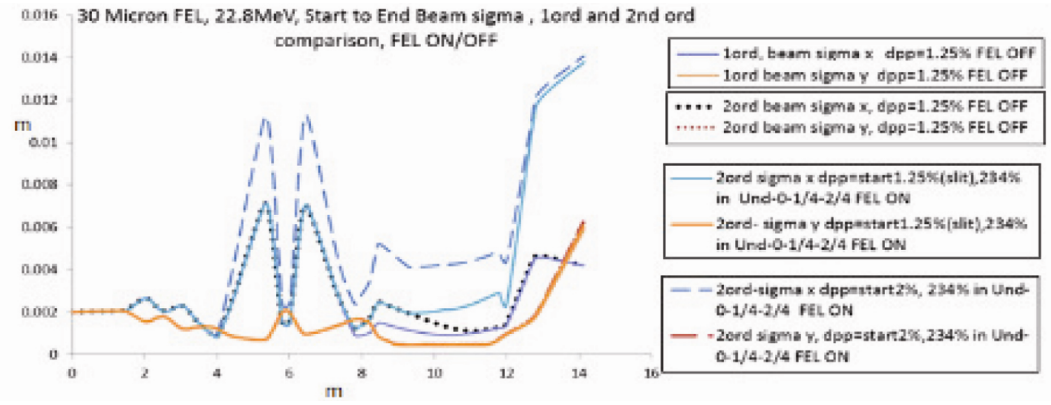

Figure 3. Results from TRANSPORT simulations showing beam sizes at different locations along the IR-FEL beam transport line.

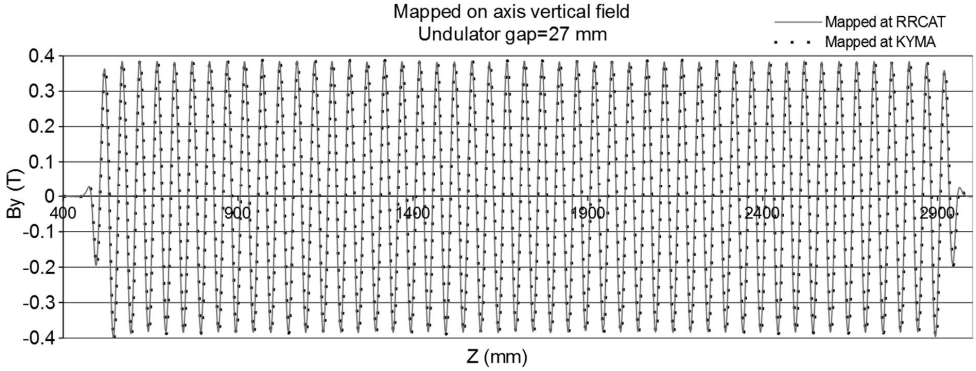

Figure 4. Undulator magnetic field profile.

Table 2. IR-FEL undulator parameters

Type	Planar, NdFeB pure permanent magnet-based
Period length (λ_u)	50 mm
RMS undulator parameter K_{RMS}	Variable, 0.5–1.2
Magnet size	12.5 × 12.5 × 50 mm^3
No. of periods (N_u)	50
Mechanical gap	Variable, 27–35 mm
$(dB)_{RMS}/\langle B\rangle$	<0.5%
Error in period	<0.05 mm (RMS), 0.1 mm (peak)
RMS phase error	<30°

in the design of the vacuum beam line, and have been used effectively to monitor and manipulate the electron beam transmission through the IR-FEL set-up. Smooth transitions have been incorporated in the vacuum beam pipe, wherever possible, between sections with different internal cross-sections to minimize the excitation of undesired beam-driven effects. The IR-FEL undulator is designed to operate with a gap of 27 mm for the design undulator parameter $K_{RMS} = 1.2$, with a specially designed vacuum chamber having a race-track internal cross-section. Special provision has been made to pump down this conductance-limited vacuum chamber to the rated vacuum level.

The vacuum system for the IR-FEL is divided into four sections: (i) injector section, (ii) beam transport line from linac exit to the optical cavity, (iii) optical cavity, and (iv) beam-dump line downstream of the optical cavity. Each section is separated from the other with the help of a gate valve to facilitate evacuation and maintenance of an individual section without affecting the vacuum in other sections.

In the injector section, the electron gun, the pre-buncher cavity and the two PWT linac structures are pumped individually by 140 l/s sputter ion pumps (SIPs). The desired vacuum level and a uniform pressure profile are maintained in the remaining three sections of the IR-FEL by employing distributed pumping with 15 SIPs, which include one 140 l/s, twelve 70 l/s and two 35 l/s capacity pumps. Based on the physics design requirements, beam pipes of different cross-sections/sizes were designed and fabricated to accommodate different shapes and sizes of the electron beam in the different sections of the beam transport line. The material of construction for all transport line elements is stainless steel (SS) of 304L grade. After the first bending magnet, a special 2040 mm long rhombus chamber having inside cross-section of 40 mm × 80 mm has been fabricated from a 2 mm thick SS 304L sheet to accommodate the maximum possible size of the beam in the available aperture of the magnet. The undulator vacuum chamber has been fabricated from an extruded aluminum alloy section to avoid any attenuation of magnetic field by the chamber material. It is a 2630 mm long chamber with a race track-type aperture of 17 mm × 81 mm. The monitoring of pressure in the complete set-up is done using eleven Bayert–Alpert (BA) gauges mounted at different locations, and the SCADA system displays the status of vacuum as well as those of all SIP power supplies on the control console in the control room.

Since the IR-FEL is installed inside a radiation shielded area, all the IR-FEL subsystems are controlled remotely through a SCADA system, which handles around 100 analog and 250 digital parameters. It monitors and controls the functioning of the following subsystems: magnet power supplies for the beam transport line magnets, RF systems (low level and high level), beam diagnostic system, undulator, vacuum system, timing and synchronization system, and the safety systems like radiation monitoring, search and secure system, access control systems, etc.

The SCADA system provides complete control of the IR-FEL set-up from the control room equipped with a control console having multiple monitors and data-logging facility with date and time stamp. The SCADA hardware is a multi-tier distributed control architecture-based on ethernet backbone. Various embedded controllers and data-acquisition hardware devices are networked using Ethernet/RS232/RS485 on subsequent layers to provide simultaneous control of various IR-FEL sub systems. The supervisory control system provides highly stable reference signals with 18-bit resolution to precisely set the current of beam transport line magnets. It provides time-synchronizing signals for the different subsystems with a timing resolution of ~10 ns. The SCADA system acquires a large number of 12/16-bit real-time parameters

from a variety of 'commercial, off-the-shelf' (COTS) instruments with diverse communication interfaces and protocols. It has provision for comprehensive data-logging and displays of on-line plots and parameters on large display walls with alarms and alerts. The electron beam diagnostic instrumentation provides real-time beam profile data, which are essential for manipulation of the beam during experiments. The SCADA system also provides hexapod controls for precise alignment of the optical cavity.

After development and offline testing of independent subsystems, installation of the different subsystems of the IR-FEL in the FEL complex was begun in June 2015. The undulator was installed at its design location and it provided the reference electron beam axis for installation of the electron beam transport line elements and the injector system. All transport line magnets and subsystems of the injector linac have been aligned to prescribed tolerance with reference to the design axis. Commissioning of the IR-FEL began with the RF conditioning of the accelerating structures with progressively increasing pulse width and peak power of the RF fed to the structures. After a period of conditioning, experiments were performed on the acceleration and transport of short, low-peak current electron bunches through the injector system and up to the dog-leg. The short electron bunches were subsequently transported through the undulator leading to the first generation of IR radiation from the set-up in January 2016. The IR radiation was measured using a liquid helium-cooled bolometer (QMC, QGeB2). Subsequent experiments on optimization of the different subsystems led to the generation of copious amounts of IR radiation from the set-up in April 2016, with the saturation of the bolometer in experiments with a 4 μs electron beam macro-pulse with ~17.6 MeV energy. The measured bolometer signal corresponds to an amplified spontaneous radiation peak power output of ~7 mW in 4 μs macro-pulse. These experiments, which marked the completion of stage-1 of commissioning experiments on the IR-FEL set-up, were performed without the downstream mirror of the optical cavity, and all the IR radiation generated through the undulator–electron beam interaction was out-coupled and measured using the bolometer.

The second stage of commissioning of the IR-FEL started with the installation of the downstream mirror of the optical cavity, followed by alignment of the optical cavity axis to match the axis of the undulator within the prescribed tolerance. The support system for this mirror includes a precision six-axis hexapod with remote operation capability for on-line alignment, and for scanning the length of the optical cavity. The downstream mirror has a 3.5 mm diameter hole for out-coupling of ~5% of the intra-cavity power. Optimization of the linac and transport line parameters resulted in a significant improvement in the beam transmission, with a measured charge of ~0.26 nC in each micro-bunch at the fourth ICT just before the undulator. This charge has an RMS energy spread of 0.75%, which is dictated by the setting of the energy-selecting slit. This was a significant improvement over the ~0.15–0.2 nC charge measured earlier during initial commissioning experiments, and is close to the desired value of 0.3 nC according to physics design simulations of the IR-FEL. The electron beam was also characterized through a measurement of its emittance using a 'quadrupole scan' method, giving a measured normalized emittance (RMS) of 40–45 mm mrad. The S-band RF system powering the two linac structures was tuned to deliver high-power microwave pulses of ~4 MW peak power to each linac structure with a flat top of ±1.25% and with a phase stability of ±2° over an 8 μs macro-pulse. This was achieved by employing a feed-forward algorithm for improvement of the amplitude and phase stability over a macro-pulse. The measured electron beam parameters during these experiments on lasing were as follows: energy = 18.2 MeV, charge per micro-pulse = 0.26 nC (giving a peak current ~26A), relative RMS energy spread = 0.75% and normalized RMS emittance = 40–45 mm mrad. With a larger length of the optical cavity compared to the design length, the bolometer output showed an out-coupled signal of ~200 mV, which corresponds to the amplified spontaneous emission generated in the undulator. The length of the optical cavity was scanned remotely in coarse/fine steps of 7 μm/2 μm during these experiments, and the out-coupled IR radiation from the IR-FEL set-up showed a steep increase in power output at a cavity length of 5038.529 mm. The estimated power gain at this cavity length is ~10^5 times compared to the expected out-coupled spontaneous radiation power for the electron beam parameters used in the experiment; this is the first signature of lasing in the IR-FEL set-up. Table 3 summarizes the electron beam and IR radiation parameters measured during these lasing experiments. Figure 5 shows a typical saturated bolometer trace during lasing.

The first signature of lasing has been successfully observed in the IR-FEL set-up with an estimated gain of ~10^5 times over expected spontaneous radiation power. The dependence of gain on the detuning length of the cavity agrees reasonably well with prediction from FEL

Table 3. Electron beam, undulator and radiation parameters during lasing

Energy	18.4 MeV
Macro-pulse width	~5 μs
Peak charge per micro-pulse (measured)	0.26 nC
Emittance (typical, measured)	~40 mm mrad (RMS, normalized)
Energy spread window chosen	~ 0.75%
Undulator gap	32 mm
Undulator parameter K_{RMS}	0.9
Wavelength of radiation (calculated)	34.4 μm
Enhancement over expected spontaneous radiation for beam parameters of the experiment	~10^5 times

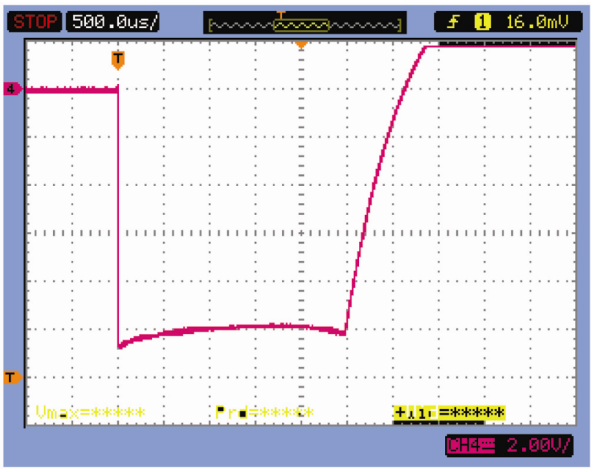

Figure 5. Typical saturated bolometer trace during lasing.

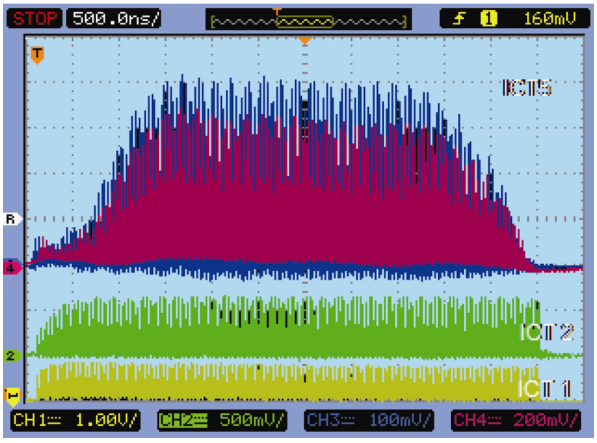

Figure 6. Integrating current transformer (ICT) trace at different locations along the beam transport line.

design simulations. These simulations also dictate a requirement of ~80 round-trips of the optical pulse inside the optical cavity for the IR-FEL to saturate through repeated interaction with electron bunches carrying ~30 A peak current. To ensure good overlap between an electron bunch and optical pulse inside the undulator, the permissible jitter in arrival time of the electron bunch at the undulator entry is ~1–2 ps, which depends critically on the stability of RF power fed to the pre-buncher and linac structures. The measured electron beam profile at the ICT at the undulator entry (Figure 6) shows a variation in the charge in each electron beam micro-pulse over a macro-pulse in the energy-selected beam, which is a manifestation of the variation in charge from the electron gun and of the RF field amplitude and phase stability in the pre-buncher and linac structures over each macro-pulse. Further, a variation in phase of RF over a macro-pulse also results in a jitter in the time of arrival of each electron beam micro-pulse at the undulator entry. Since the time of arrival of the optical pulse at the undulator entry after each round-trip inside the optical cavity is fixed, this jitter in electron bunch arrival results in poor overlap between the electron and optical pulses causing a drop in gain for that pass number. In order to achieve saturation, the stability of the injector system needs to be further improved through an improvement in the amplitude and phase stability of the RF powering the pre-buncher and linac structures.

Injector design simulations point to a requirement of 0.1% amplitude stability and 0.15° phase stability in the pre-buncher RF, and 0.1% amplitude and 1° phase stability in the S-band power for the linac structure. Experiments are presently underway for improving the performance of the injector subsystems to achieve saturation in the IR-FEL, which will lead to a gain of ~10^7 with a peak out-coupled power of 2 MW and a CW average power output of ~30 mW at 10 Hz operation.

1. Cohn, K., Blau, J., Colson, W. B., Ng, J. and Price, M., Free electron lasers in 2015. In Proceedings of Free Electron Laser Conference, Korea, 23–28 August 2015, p. 625.
2. Kumar, V. *et al.*, Design of an infra-red free electron laser at RRCAT. In Proceedings of InPAC, IUAC, New Delhi, 2011.
3. Kumar, A., IRFEL injector simulations. In Proceedings of InPAC 2009, RRCAT, Indore, 2009.
4. Kumar, G. *et al.*, Installation, testing and commissioning of 10 kW pulse RF amplifier system @ 476 MHz using planar triode for IRFEL. In Proceeding of InPAC 2015, TIFR Mumbai, 2015; Tiwari, N. *et al.*, Development and deployment of CW and pulse digital low level RF systems for accelerators at RRCAT. In Proceeding of InPAC 2015, TIFR Mumbai, 2015.
5. Praveen, M. *et al.*, Design and development of low level S-band RF control system for IRFEL injector Linac. In Proceeding of InPAC 2015, TIFR Mumbai, 2015; Shrivastava, P., Status of 24 MW microwave system and LLRF control for IR-FEL linac. *RRCAT Newsl.*, 2016, **29**(1).
6. Singh, A. *et al.*, Power supplies for IRFEL beam transport line magnets. In Proceeding of InPAC 2015, TIFR, Mumbai, 2015.
7. Saini, R. S. *et al.*, Electron beam optics design of variable energy beam transport line for a tunable infra-red free electron laser at RRCAT. In Proceedings of InPAC 2011, IUAC, New Delhi, 2011.
8. Enomoto, A. and Dael, A., Technical Report – Lure Anneaux TF.CLIO/88-02 et CERA. 88-97/CLIO, Orsay, France, 19 May 1988.
9. Kailash, R. *et al.*, Development of magnets for infra-red free electron laser project at RRCAT. In Proceeding of InPAC 2015, TIFR Mumbai, 2015.

ACKNOWLEDGEMENTS. We acknowledge the unstinted support and continued guidance received from Dr S. B. Roy from the planning stage of the project to the first lasing of the IR-FEL. The authors from MAASD acknowledge several fruitful scientific discussions with him at various stages of the design, development and implementation of some of the IR-FEL subsystems. We thank Dr P. D. Gupta (RRCAT, Indore) and Dr P. A. Naik (Director, RRCAT) for their support and encouragement. We acknowledge the help and support received from different Divisions of RRCAT for development of subsystems of the IR-FEL. Technical assistance of Mr. Rajkumar B. Bhowate during installation of the IR-FEL set-up is acknowledged.

Received 22 July 2017; accepted 9 August 2017

doi: 10.18520/cs/v114/i02/367-373